

Ultrasimple calculation of very-low-energy momentum-transfer and rotational-excitation cross sections: e - N_2 scattering

Michael A. Morrison, Weiguo Sun,* William A. Isaacs, and Wayne K. Trail

Department of Physics and Astronomy, University of Oklahoma, Norman, Oklahoma 73019-0225

(Received 24 May 1996)

The calculation of electron-molecule cross sections at scattering energies well below 0.1 eV using conventional algorithms for solving the Schrödinger equation is often rendered problematic by severe numerical problems. Here we describe and implement an alternative procedure that combines known analytic properties of the body-frame electron-molecule scattering matrix, as codified in the modified effective range theory, with an analytic correction that imposes physically correct threshold laws. This approach eliminates completely the need for numerically solving the Schrödinger equation at energies below about 0.1 eV. Instead, one uses scattering matrices above this energy to determine parameters for an extrapolation to subthermal energies. We apply this method to the calculation of e - N_2 momentum-transfer and rotational excitation cross sections from threshold to 1.25 eV. The results resolve a long-standing apparent anomaly in the analysis of experimental data for very low-energy electron scattering from N_2 . Finally, we use linear regression to present our theoretical results in a user-friendly form. [S1050-2947(97)08603-4]

PACS number(s): 34.80.Gs

I. INTRODUCTION

Integral elastic, momentum transfer, and rotational excitation cross sections at energies below 0.1 eV are of interest not only for the fundamental insight they afford into quantum dynamics, threshold behavior, and many-body effects such as bound-free correlation, but also for technological applications. These range from the modeling and optimization of plasma devices and gas lasers to understanding planetary atmospheres and photoelectric heating in astrophysics. Because rotational energy levels are very closely spaced (with typical separations on the order of meV) and very many levels are populated under common physical (and experimental) conditions [e.g., experiments at room temperature (293 K) excite roughly 20 rotational states of N_2 [1]], such applications often require a huge number of rotational cross sections. These concerns further highlight the need for efficient, numerically reliable ways to calculate the rotational cross sections that participate in energy transfer in low-temperature molecular gases. One such method is the subject of the present work.

Recent advances in experimental techniques for measuring electron-molecule cross sections have heightened interest in scattering at energies well below 0.1 eV—the very-low-energy (VLE) region. Prominent among these advances are the use of afterglow and drift tube techniques [2], electron monochromators [3], monoenergetic electrons resulting from photoionization of rare-gas atoms [4], and Rydberg atoms. The latter, excited to states with principal quantum number from several hundred to over 1000, serve as a VLE electron trap in collisions with molecules [5]. A survey of these advances can be found in the topical review by Dunning [6]

and subsequent developments in the report of a recent conference on VLE scattering [7].

Such techniques complement the indirect determination of cross sections by Boltzmann analysis of data taken in swarm experiments. This swarm data directly yields transport coefficients—collective properties of the swarm of electrons as it drifts and diffuses through a dilute gas of molecules of known density and temperature under the influence of an applied electric field of known strength. Transport analysis then seeks to reproduce these data from an electron velocity distribution function determined by solving the Boltzmann equation with an assumed set of cross sections as input [8,9]. The analysis is iterative, the cross sections being varied until self-consistency is attained between calculated and measured transport coefficients. Swarm experiments, too, have advanced in recent years, notably in a new class of such experiments based on direct production of the electron swarm by a short UV laser pulse [10]. As documented in the monograph by Huxley and Crompton [11] and in recent reviews [12], transport analysis is now well established as the primary—and for many systems the sole—source of integral rotational, vibrational, and momentum transfer cross sections at energies below several tenths of an eV. Since 1979, we have been collaborating with crossed-beam and swarm experimentalists to subject these cross sections to close scrutiny in conjunction with *ab initio* theoretical cross sections of high numerical precision [13–15]. To date this effort has focused on e - H_2 scattering [9,13,14].

This program has now turned to the scattering of VLE electrons by N_2 . Boasting a more complicated electronic structure and far more strongly nonspherical static field than H_2 , as well as an intermediate duration shape resonance at 2.39 eV, the e - N_2 system has become the prototype for testing both theoretical and experimental approaches to resonant and nonresonant low-energy collisions [15]. For a review of the extensive theoretical literature on this system, see Ref. [16]; for resonant scattering, see Ref. [17]; for experimental

*Permanent address: Department of Chemistry, The Sichuan Union University, Chengdu, Sichuan 610065, People's Republic of China.

results, see Ref. [18]; and the data compilation Ref. [19].

We have selected e - N_2 scattering for the present study in hopes of gaining insight into a long-standing enigma concerning VLE rotational excitation in this system. Transport analysis of e - N_2 swarm data requires as input $j_0 \rightarrow j_0 \pm 2$ rotational cross sections for all initial rotational states j_0 populated in the target gas. From the earliest such analyses to the most recent [20–22], experimentalists have calculated these cross sections using the simple quadrupole Born approximation (QBA) expression derived by Gerjuoy and Stein [23]. In the essential role of this expression lies the enigma.

The QBA expansion is valid *in the threshold limit* where the exit channel projectile wave number $k_j \rightarrow 0$. Just above threshold, however, the long-range r^{-4} (induced) polarization interaction becomes important. Not surprisingly, the quadrupole-polarization Born approximation (QPBA) expression of Dalgarno and Moffett [25] deviates substantially from the QBA form. With still further increases in energy, intermediate- and short-range interactions (static, exchange, nonasymptotic polarization, and correlation) begin to affect the scattering, and the weak scattering assumption of the Born approximation rapidly breaks down [26]. All this appears to happen within a few tens of meV of threshold, well below the characteristic energy of the swarms in the aforementioned experiments. *Yet only the QBA cross section—not the presumably more accurate QPBA results nor cross sections from theoretical studies that include short- and intermediate-range interactions [27,28]—yield transport coefficients within the 1% error bars on the measured data.* A desire to understand more fully the physics of VLE rotational excitation, to resolve this conundrum, and to produce a data base of numerically sound $|\Delta_j|=2$ cross sections that reflect the full e - N_2 interaction motivated the present research, which complements a recent analysis of transport data taken in swarm experiments in N_2 - Ne mixtures [29].

The challenge VLE scattering poses to the theorist is that solving the electron-molecule Schrödinger equation at energies below a few tenths of an eV entails a host of sometimes severe practical difficulties. In methods based on a single-center expansion of the scattering function in angular momentum eigenstates of the projectile [30,16], these difficulties arise predominantly from the strongly nonspherical interaction potential. This potential is dominated by the short-range electron-nuclear Coulomb interaction and so can strongly couple a large number of partial waves—projections of the scattering function on spherical harmonics defined with respect to an origin of coordinates at the center of mass of the molecule. Because of repulsive centrifugal potentials in scattering channels with projectile orbital angular momenta $\ell > 0$, many of these strongly coupled radial functions decay rapidly as $r \rightarrow 0$. This decay is exacerbated with decreasing energy, since as the classical turning point in each channel rapidly grows, so does the size of the classically forbidden region.

Consequently, a host of unsightly technical problems bedevil the numerical solution of the Schrödinger equation at very low energies. These include a breakdown of linear independence among the columns of the radial wave-function matrix, accelerating error in propagating this matrix through the strong potential region because of the extreme range of magnitudes in various channel components, and (in algo-

rithms based on the integral form of the Schrödinger equation) difficulties attendant upon generating the channel Green's functions needed to impose scattering boundary conditions [31,32]. Even if these problems are not crippling, one realizes that the growing number of partial waves required as the energy descends into the VLE region is a nonphysical artifice—a mathematical consequence of the off-center singularity in the (fixed-nuclei) electron-nuclear static potential. Our present goal is to avoid completely such scattering calculations.

To this end we offer in Sec. II a procedure that exploits the known analytic properties of the scattering matrix, as embodied in modified effective range theory (MERT), and approximate treatments of the rotational dynamics that ensure physically correct (PC) threshold behavior of VLE cross sections. This procedure follows the MERT philosophy of analytically “extrapolating” scattering quantities to very low energy; here we extrapolate elements of the scattering matrix from energies above 0.1 eV, where they can be calculated with relative ease by numerical solution of the Schrödinger equation, into the VLE region. This procedure involves minimal computational effort, requiring only a few seconds on a personal computer. Following a sketch of the method and a summary of its key equations in Sec. II we apply it to e - N_2 scattering at energies from zero to several tenths of an eV in Sec. III. In a companion experimental and theoretical paper [29], these results are used in transport analysis of e - N_2 swarm data.

II. THEORY AND IMPLEMENTATION

Here we describe our procedure for calculating VLE cross sections for electron scattering from a closed-shell nonpolar molecule. The context for this method—the close-coupling solution of the nonrelativistic Schrödinger equation for this collision system—has been reviewed several times previously [16–34]; the review of Shimamura [34] is devoted solely to rotational excitation, and emphasizes sum rules and scaling relations. Equations for close-coupling solution of the scattering equations in the present formalism appear in the review by Morrison and Sun [35], and will not be repeated here. Additional background concerning our implementation of these equations to e - N_2 scattering can be found in Ref. [15]. Finally, we discussed application of the body-frame-modified effective range theory formalism of Fabrikant [36] to the calculation of VLE *total* cross sections in Ref. [37].

A. Overview of procedure

Three theoretical assumptions underlie the method used here. First, at energies below about 0.1 eV, we can approximate scattering matrix elements of low partial wave order by analytic expansions in powers of the exit channel electron wave number (MERT). Second, we can approximate elements of high partial wave order using the first Born approximation (FBA) [32,38]; the validity of this assumption hinges on scattering in these channels being weak and due to the long-range interaction potential. Third, we can treat the rotational motion adiabatically, subject to a correction that ensures a PC dependence of the scattering matrix on energy near threshold.

The assumption of adiabatic rotations inheres in the fixed nuclear orientation (FNO) approximation, according to which the orientation \hat{R} of the internuclear axis is fixed during the collision [16]. This approximation, which eliminates the rotational Hamiltonian from the Schrödinger equation, is valid except at scattering energies that are comparable to the rotational level spacing of the target [30,33]. The solution of the FNO Schrödinger equation (subject to real boundary conditions) yields a reactance (K) matrix that describes the projectile dynamics but not target rotational excitation. This K matrix is subsequently transformed to a transition (T) matrix appropriate to the scattering process of interest.

Rotations are reintroduced asymptotically via a rotational frame transformation of the T matrix [39]. But the resulting rotationally inelastic T -matrix elements approach a positive constant rather than zero as the energy approaches threshold. This defect in the FNO formulation, if left uncorrected, generates enormous errors in VLE rotational cross sections [32]. We impose PC near-threshold behavior on the frame transformed T matrix using the scaled adiabatic nuclear rotation (SANR) theory summarized below [40].

Prior to invoking the frame transformation, we work entirely within the FNO approximation. Hence we conveniently express the Schrödinger equation in a body-fixed (BF) reference frame whose z axis is coincident with \hat{R} . In addition to reintroducing rotations, the rotational frame transformation also transforms the T matrix from the body frame to a space-fixed frame appropriate to the laboratory description of the collision.

Our procedure for calculating the BF K matrix depends on whether the scattering energy is above or below the ‘‘boundary energy’’ E_M : for $E \geq E_M$ we solve coupled radial scattering equations using a static-exchange-polarization (SEP) interaction potential and including the full complement of partial waves required to converge the scattering quantity of interest (usually, these are key K -matrix elements) to 1% or better [15]. For $E \leq E_M$ we use the simple analytic BF MERT expressions given in Sec. II B. The connection between these two energy regions is made via parameters in the MERT equations, which we determine from K -matrix elements at a few energies $E \geq E_M$. This procedure, along with the implementation of the other two underlying assumptions, is summarized in Fig. 1. In the rest of this section, we present relevant equations and specifics of their application to e - N_2 scattering.

B. Modified effective range theory

The fundamental equations of modified effective range theory (MERT) are analytic expansions of various scattering quantities in powers of the exit-channel projectile wave number [41–46]. These expansions do not depend on the many assumptions and approximations that typically underlie scattering calculations (e.g., the representation of the target, approximations to the interaction potential, or assumptions about the dynamics). Rather, they are based on analytic properties of the S matrix near threshold [42].

For electron-atom and electron-molecule scattering, MERT extends the familiar effective range theory for short-range potentials [47], so as to accommodate long-range interactions such as the spherically symmetric $1/r^4$ -induced

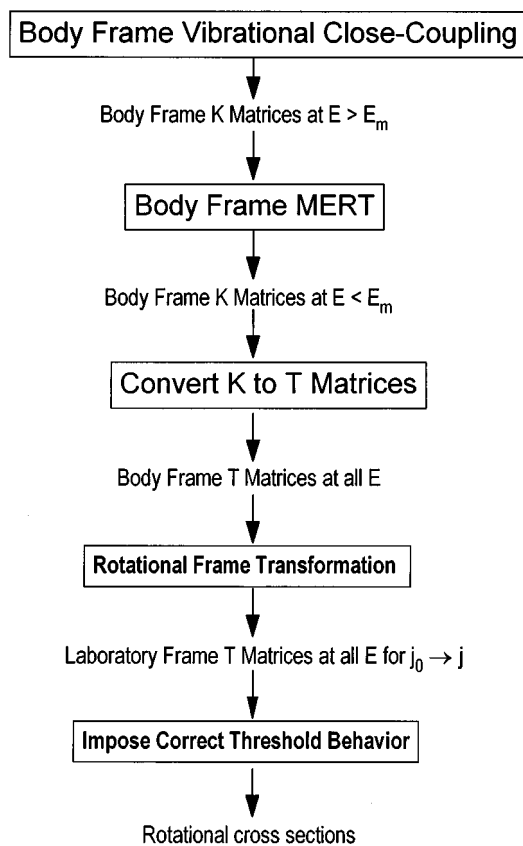


FIG. 1. Summary of MERT extrapolation procedure for calculating rotational cross sections.

polarization potential characteristic of both types of systems [43]. For electron-molecule scattering, MERT must also take into account the non-spherical long-range polarization and permanent quadrupole potentials [44,42,33].

These potentials depend only on the permanent and induced moments of the target, averaged over the probability density of the ground vibrational state. For a homonuclear target, these are the spherical and nonspherical polarizabilities $\bar{\alpha}_0$ and $\bar{\alpha}_2$, and the (permanent) quadrupole moment \bar{Q} :

$$\bar{\alpha}_\lambda = \langle \phi_0^{(v)} | \alpha_\lambda | \phi_0^{(v)} \rangle \quad (\lambda = 0, 2),$$

$$\bar{Q} = \langle \phi_0^{(v)} | Q | \phi_0^{(v)} \rangle, \quad (1)$$

where the overbar denotes the average over the ground vibrational wave function $\phi_0^{(v)}(R)$. The long-range potential is then

$$V_{\text{int}}(r, \theta) \sim -\frac{\bar{\alpha}_0}{2r^4} - \left[\frac{\bar{Q}}{r^3} + \frac{\bar{\alpha}_2}{2r^4} \right] P_2(\cos \theta), \quad (2)$$

where θ is the scattering angle in the body frame. These three moments appear in the leading terms in MERT expansions along with one or more parameters intended to incorporate short- and intermediate-range interactions that influence VLE collisions. These interactions affect primarily s -wave channels, and their effects are usually collapsed into

a single parameter, the scattering length A , which characterizes the scattering function in the zero-energy limit [47].

Expansions of the K -matrix elements in the BF FNO formulation of electron scattering from a closed-shell nonpolar molecule were derived by Fabrikant [36] using MERT, and have been implemented by Isaacs and Morrison [37] for low-energy total e -H₂ and e -N₂ cross sections. In the BF FNO formulation, elements of scattering matrices are labeled by channel quantum numbers $(\nu, \ell; \Lambda)$, where ν signifies the vibrational state of the target, ℓ the orbital angular momentum of the projectile, and Λ its projection along $\hat{z} = \hat{R}$. In the FNO approximation, Λ is a constant of the motion, so the radial scattering equations are uncoupled in Λ ; for homonuclear targets, parity η is also conserved. Hence the K matrix is block diagonal, and the collision is (colloquially) described as occurring in independent electron-molecule symmetries labeled $\Sigma_g(\Lambda=0, \text{even parity})$, $\Sigma_u(\Lambda=0, \text{odd})$, $\Pi_u(\Lambda=1, \text{odd})$, etc. We shall denote particular elements of this matrix by appending orbital quantum numbers onto the symmetry designation: e.g., $\Sigma_g(2,0)$ denotes the element of the Σ_g K matrix with $\ell=0$ and $\ell_0=2$. As we are interested here in vibrationally elastic collisions ($\nu = \nu_0 = 0$) we shall suppress the vibrational quantum number ν and write K -matrix elements as $K_{\ell, \ell_0}^{\Lambda, \eta}$. At energies above E_M , we extract these elements from converged solutions to the body frame vibrational close-coupling scattering equations [15,35,48], which we solve using an integral equations algorithm [49–51], as described in Ref. [35].

For $E < E_M$ we use the MERT expansion of $K_{\ell, \ell_0}^{\Lambda, \eta}$ in powers of the projectile wave number

$$k = \sqrt{2m_e E}. \quad (3)$$

To order k^3 , this expansion is

$$K_{\ell, \ell_0}^{\Lambda, \eta} = c_1 k + c_2 k^2 + Z_{\ell, \ell_0}^{\Lambda} k^3 \ln k + O(k^3). \quad (4)$$

The linear and k^2 coefficients are

$$\begin{aligned} c_1 &= -A \delta_{\ell_0} \delta_{\ell_0} + \bar{Q} q_{\ell, \ell_0}^{\Lambda(1)}, \\ c_2 &= \bar{\alpha}_0 a_{\ell} \delta_{\ell, \ell_0} + \bar{\alpha}_2 (-1)^{\ell + \Lambda} \begin{pmatrix} \ell & \ell_0 & 2 \\ \Lambda & -\Lambda & 0 \end{pmatrix} \\ &\quad \times p_{\ell, \ell_0} + \bar{Q}^2 q_{\ell, \ell_0}^{\Lambda(2)}, \end{aligned} \quad (5)$$

with

$$a_{\ell} = \frac{\pi}{(2\ell - 1)(2\ell + 1)(2\ell + 3)}. \quad (6)$$

Analytic expressions for the other factors in Eq. (5)— $q_{\ell, \ell_0}^{\Lambda(1)}$, $q_{\ell, \ell_0}^{\Lambda(2)}$, p_{ℓ, ℓ_0} , and $Z_{\ell, \ell_0}^{\Lambda}$ —can be found in Ref. [36].

Of particular importance in the application of BF MERT to rotational excitation are restrictions in Eqs. (4)–(6) on the orbital angular momenta and the presence or absence in c_1 and $Z_{\ell, \ell_0}^{\Lambda}$ of the scattering length A . First, Wigner $3j$ coefficients in $q_{\ell, \ell_0}^{\Lambda(1)}$ and $q_{\ell, \ell_0}^{\Lambda(2)}$ restrict the change in angular momentum in the collision to $\Delta\ell = \ell - \ell_0 = \pm 2$. Hence the

present method is applicable only to rotational excitations $j_0 \rightarrow j = j_0 \pm 2$. Second, short-range effects influence $Z_{\ell, \ell_0}^{\Lambda}$ only for two elements of the Σ_g symmetry: $\Sigma_g(0,0)$ and $\Sigma_g(2,0)$. As we shall see in Sec. III, this dependence is crucial to VLE scattering. [For other elements of the Σ_g K matrix, and those of other symmetries, the MERT expansion Eq. (4) through order k^2 is identical to the first Born approximation expression based on the asymptotic interaction potential Eq. (2); see the Appendix to Ref. [32].]

For rotational excitation with $\Delta j = 2$, the key element of the BF K matrix is $\Sigma_g(2,0)$. The corresponding Z coefficient depends on A as

$$Z_{0,2}^0 = \frac{1}{105\sqrt{5}} \left[\frac{2}{3} \bar{Q}^3 + \frac{14}{3} \bar{\alpha}_0 \bar{Q} - 5 \bar{\alpha}_2 \bar{Q} + A(2\bar{Q}^2 + 7\bar{\alpha}_2) \right]. \quad (7)$$

Because this coefficient multiplies $k^3 \ln k$ in Eq. (4), this A dependence may (and, for VLE e -N₂ scattering, does) inadequately represent the influence on scattering in the Σ_g symmetry from regions of space near the target. We can extend the range of validity of the expansion Eq. (4) by including higher-order coefficients, as

$$K_{\ell, \ell_0}^{\Lambda, \eta} = c_1 k + c_2 k^2 + Z_{\ell, \ell_0}^{\Lambda} k^3 \ln k + c_3 k^3 + c_4 k^4 + O(k^5). \quad (8)$$

The additional coefficients c_3 and c_4 incorporate short- and intermediate-range effects beyond those represented by the scattering length A . Since physically based expressions such as Eqs. (5) do not exist for these coefficients, they should be considered mere numerical fitting parameters.

The use of such expansions immediately raises questions about the range of their validity [46]. Although MERT is formally valid in the threshold limit $k_j \rightarrow 0$, in practice its expansions remain accurate well above this limit. Hence their range of validity must be determined empirically for each system and symmetry class [37]. This is an issue of great importance, because in our procedure we extract the scattering length (and, if required, parameters c_3 and c_4) from BFVCC K -matrix elements at energies above E_M , and at these energies MERT must be valid. In practice, we have found the BF MERT theory for rotational excitation summarized in Fig. 1 to be valid to 1% for e -N₂ scattering at energies up to 0.4 eV and, in independent studies (not shown), for e -H₂ scattering up to 0.3 eV.

C. Interaction potential

The electron-molecule interaction potential in the BFVCC equations for $E \geq E_M$ contains static, exchange, and correlation-polarization terms [16,30]. The e -N₂ potential used in the present calculations has been described in detail elsewhere [15], so we shall only summarize its high points.

The static and exchange terms are based on an R -dependent Hartree-Fock (single-configuration) wave function for the ground X ¹ Σ_g electronic state of N₂. To generate the correlation-polarization potential, we augment the Hartree-Fock basis with diffuse functions that allow for polarization distortions [52]. From the asymptotic form of the

TABLE I. Permanent and induced moments of N_2 used in the MERT expressions for body-frame K -matrix elements; see also Ref. [53].

Source	$Q(ea_0^2)$	$\alpha_0(a_0^3)$	$\alpha_2(a_0^3)$
Present theory	-0.9608	10.980	3.096
Experiment	-1.09 ± 0.07^a	11.744 ± 0.004^b	3.08 ± 0.002^c
CI target function	-1.14^d	11.52^e	3.16^e

^aFrom induced optical birefringence measurements by Buckingham, Graham, and Williams (Ref. [54]).

^bMeasured by Orcutt and Cole (Ref. [55]) and Newell and Baird (Ref. [56]).

^cFrom relative anisotropies of Bridge and Buckingham (Ref. [57]).

^dMany-body perturbation results of Cernusak, Dierksen, and Sadles (Ref. [58]).

^eMultireference CI results of Langhoff, Bauschlicher, and Chong (Ref. [59]).

static potential at each R , we extract the quadrupole moment function $Q(R)$ and from the long-range polarization potential, the spherical and nonspherical induced polarizability functions $\bar{\alpha}_0(R)$ and $\bar{\alpha}_2(R)$. We then average these functions over the ground vibrational state, using Morse vibrational functions as described in Ref. [15], obtaining the values in Table I. These quantities appear in the MERT coefficients (5).

Finally we note two approximations in our interaction potential. First, we treat short-range nonlocal bound-free correlation effects using the nonpenetrating approximation of Temkin [60]. This results in a parameter-free local correlation-polarization potential that, for reasons detailed elsewhere, we call the ‘‘better-than-adiabatic dipole’’ potential [28,61]. Second, we approximate exchange effects using a parameter-free energy-dependent local potential based on the free-electron-gas model originally introduced to electron-molecule scattering by Hara [62]. While this potential has been exhaustively studied for various electron-molecule systems [63], it must be extensively modified to accommodate e - N_2 scattering as described in Ref. [15].

D. From the K matrix to rotational cross sections

To address the issues raised in Sec. I concerning transport analysis of e - N_2 swarm data, we require a total momentum transfer $\sigma^{(m)}$ and rotational excitation cross sections $\sigma_{j_0 \rightarrow j}^{(r)}$. These we calculate from BF FNO K matrices, which we obtain either from solutions of the BFVCC scattering equations for $E > E_M$, or from MERT expansions for $E < E_M$. One can, of course, use analogous MERT expansions to calculate total integral and differential cross sections [37]. The cross sections $\sigma^{(m)}$, which can easily be generated from the BF FNO K matrix, using Eq. (136) in [35], includes contributions from elastic scattering and rotational excitation for all open channels. Calculating the rotational cross section from the K matrix requires that we first transform this matrix into a T matrix in a space-fixed laboratory frame whose z axis is coincident with the incident electron wave vector \mathbf{k}_0 . This transformation [39] alters the representation from BF FNO theory, in which asymptotic channels are labeled by $(\nu, \ell; \Lambda)$, to the laboratory-frame coupled angular momen-

tum (LAB-CAM) theory, in which channels are labelled $(\nu, j, \ell; J)$ with j the rotational quantum number of the target and J the total angular momentum of the system.

This transformation is implemented in two steps. First we transform the BF FNO K matrix into a T matrix in the same representation via the transformation

$$\mathsf{T}^\Lambda_\eta = -2i\mathbf{K}^\Lambda_\eta(\mathbf{1} - i\mathbf{K}^\Lambda_\eta)^{-1}, \quad (9)$$

where the prefactor $-2i$ corresponds to the convention $\mathsf{T}^\Lambda_\eta = \mathbf{1} - \mathbf{S}^\Lambda_\eta$. Second we transform the BF FNO T matrix to the LAB-CAM representation via the unitary rotational frame transformation [39]

$$T_{j\ell, j_0\ell_0}^J = \sum_\Lambda A_{j\ell}^{J\Lambda} T_{\ell, \ell_0}^{\Lambda\eta} A_{j_0\ell_0}^{J\Lambda}, \quad (10)$$

where

$$A_{j\ell}^{J\Lambda} = \left(\frac{2j+1}{2J+1} \right)^{1/2} C(j\ell J; \Lambda, -\Lambda), \quad (11)$$

with the conventions of Rose for the Clebsch-Gordan coefficients [64]. This second transformation reintroduces the rotational dynamics to the asymptotic description of the collision, as required to describe transitions $j_0 \rightarrow j$; physically, this procedure is equivalent to the adiabatic nuclear rotation approximation [65].

At energies near a rotational threshold ϵ_j , we must invoke an additional correction because rotational cross sections calculated directly from the LAB-CAM T matrices that emerge from the transformation (10) do not obey PC threshold laws. That is, these cross sections behave incorrectly as the exit-channel wave number k_j approaches zero, where

$$k_j \equiv \left(\frac{2m_e}{\hbar^2} (E - \epsilon_j) \right)^{1/2}, \quad (12)$$

with m_e the electron mass and ϵ_j the threshold energy measured from the ground rotational state. In terms of the rotational constants B_0 and D_0 , this threshold energy is [66]

$$\epsilon_j = B_0 j(j+1) - D_0 j^2(j+1)^2. \quad (13)$$

Specifically, elements of the LAB-CAM T matrix must go to zero according to a power law [67,33,32] that depends on ℓ , the order of the dominant partial wave (in the exit channel) at energy E :

$$T_{j\ell, j_0\ell_0}^J \underset{k_j \rightarrow 0}{\sim} k_j^{\ell+1/2}. \quad (14)$$

This, in turn, forces the cross section to zero as

$$\sigma_{j_0 \rightarrow j}^{(r)} \underset{k_j \rightarrow 0}{\sim} k_j^{2\ell+1}. \quad (15)$$

However, rotationally frame-transformed T -matrix elements do not obey Eq. (14), and cross sections calculated from them do not obey Eq. (15); in fact the latter approach a nonzero constant at threshold.

To ensure that all LAB-CAM T -matrix elements that are important to the cross sections of interest conform to the

threshold law (14), we scale the results of the rotational frame transformation (10) by a ratio of matrix elements calculated in the first Born approximation [40]. Details of this “scaled adiabatic nuclear rotation” correction appear as Eqs. (140) and are discussed in Ref. [35]; the required Born matrix elements can be found in the Appendix to Ref. [32] and in Sec. III A of Ref. [15]. As we shall demonstrate in Sec. III, rotational cross sections calculated from corrected T -matrix elements do approach zero according to Eq. (15). This consideration is particularly important for transport analysis of swarm data in e -N₂, because the electron velocity distribution is quite sensitive to rotational excitation from threshold to 0.1 eV. (The rotational threshold of N₂ is very small owing to the small rotational constant $B_0=1.998$ cm⁻¹; for the 0→2 excitation, for example, the threshold is 1.479 89 meV.) For this system we apply this correction at energies below 0.2 eV.

Having generated and, if necessary, corrected the LAB-CAM T matrices, we can calculate the desired rotational cross sections, which are sums over final and averages over initial rotational sublevels m_j and m_{j_0} . To facilitate the analysis of our results in Sec. III, we write these quantities as sums over cross sections partial in the total angular momentum quantum number J ,

$$\sigma_{j_0 \rightarrow j}^{(r)} = \frac{1}{2j_0+1} \sum_{J=0}^{\infty} (2J+1) \sigma_{j_0 \rightarrow j}^J. \quad (16)$$

These J partial cross sections can in turn be decomposed according to the partial waves of the projectile in the entrance and exit channels, as

$$\sigma_{j_0 \rightarrow j}^J = \sum_{\ell, \ell_0} \sigma_{j_0 \rightarrow j}^J(\ell_0 \rightarrow \ell), \quad (17)$$

which, finally, are related to the T matrix as

$$\sigma_{j_0 \rightarrow j}^J(\ell_0 \rightarrow \ell) = \frac{\pi}{k_0^2} |T_{j', j_0 \ell_0}^J|^2. \quad (18)$$

Two special features of the cross-section calculation at very low scattering energies deserve note. First, the sum over Λ in the rotational frame transformation (10) includes all electron-molecule symmetries allowed by the triangle rules imposed by the Clebsch-Gordan coefficients in Eq. (11). Depending on the values of ℓ and ℓ_0 for the LAB-CAM T matrix being generated, these sums over Λ may call for BF FNO K -matrix elements $K_{\ell, \ell_0}^{\Lambda}$ that were not obtained in the BFVCC (or MERT) scattering calculations, because these calculations are typically performed only for small- Λ symmetries. For example, even at energies below several tenths of an eV, we find that to converge $\Delta j=2$ rotational cross sections for e -N₂ we must include LAB-CAM matrix elements with $\ell \geq 2$. To generate these via Eq. (10) requires, in turn, BF FNO K -matrix elements with $\Lambda > 1$. Rather than perform additional BFVCC calculations for such high- Λ symmetries, we approximate the required K matrices using the first Born approximation in the BF FNO formulation [32]; for e -N₂ scattering below several tenths of an eV, this approximation is quite accurate for $\ell \geq 2$.

TABLE II. MERT parameters (in atomic units) obtained via a least-squares fit to BFVCC K matrices at 0.1, 0.12, 0.16, 0.18, and 0.20 eV. Also shown (in parentheses) are MERT parameters for a rigid-rotor calculation at $R=2.068a_0$.

K -matrix element	A	c_3	c_4
$\Sigma_g(0,0)$	0.420 (0.483)	29.148 (27.650)	-57.919 (-57.260)
$\Sigma_g(2,0)$		-0.926 (-2.270)	-5.884 (-4.903)
$\Sigma_g(2,2)$		1.391 (2.222)	-6.409 (-12.934)

Second, we must face a similar problem in evaluating the sum over J in the final rotational cross section (16). In practice this sum runs not to infinity but rather to some finite maximum value J_{\max} determined to ensure convergence to the desired accuracy. For each included J , the partial cross section $\sigma_{j_0 \rightarrow j}^J$ is calculated from Eq. (17) by summing over partial-wave orders ℓ and ℓ_0 as prescribed by the triangle rules $\Delta(j_0 \ell_0 J)$ and $\Delta(j \ell J)$. These partial wave sums typically call for T -matrix elements whose order exceeds the maximum generated in the BFVCC or MERT scattering calculations. If this happens, we again invoke the first Born approximation—this time in the LAB-CAM formulation; this strategy is justified for e -N₂ scattering in Sec. IV C of Ref. [15]. To converge the present cross sections, for example, we require LAB-CAM T -matrix elements of orders up to $\ell=10$; those for $\ell > 2$ we replace with their first Born approximates.

III. RESULTS AND DISCUSSION

In this section we use the MERT extrapolation procedure to calculate VLE rotational and momentum transfer cross sections for e -N₂ scattering, then use the results to explain the seemingly anomalous behavior of $\sigma_{0 \rightarrow 2}^{(r)}$ in transport analysis for nitrogen. To demonstrate the accuracy of this procedure, we first compare MERT-extrapolated K -matrix elements and cross sections to those from converged solutions of the BFVCC scattering equations. We preface this demonstration with a few remarks on implementation of the procedure.

The first step is determining the parameters in the MERT expansions for the requisite K -matrix elements. For example, for elements in the Σ_g symmetry, we calculated A , c_3 , and c_4 via a least-squares fit to BF-FNO K -matrix elements obtained from solutions of the BFVCC scattering equations at energies $E \geq E_M$. In particular, to obtain the values in Table II, we used 0.1, 0.12, 0.16, 0.18, and 0.20 eV. Our choice of these energies as input to the least-squares fit, although somewhat arbitrary, is guided by two criteria. First, the MERT expansion must be valid at all energies used in the fit. Second, BFVCC scattering calculations must be computationally viable at these energies. We expect $E_M=0.1$ eV to be reasonable for many electron-molecule systems: at and above this energy, solution of the scattering equations is nu-

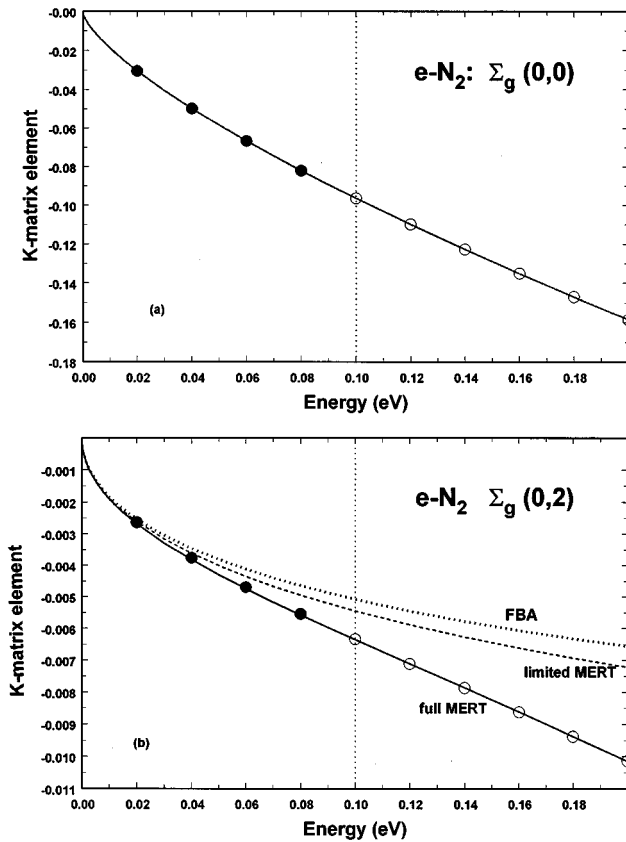


FIG. 2. MERT extrapolations (solid curve) of the (a) $\Sigma_g(0,0)$ and (b) $\Sigma_g(2,0)$ elements of the $e\text{-N}_2$ K matrix for vibrationally elastic scattering. The BFVCC K -matrix elements are shown at $E \geq 0.1$ eV (open circles)—these were used to determine the MERT parameters—and at a few energies below E_M (solid circles) for comparison to the MERT extrapolation. In (b) the “full MERT” extrapolation Eq. (8), which yielded the solid curve, included terms through k^4 , with parameters as in Table II. This is to be compared to the “limited MERT” extrapolation (dashed curve) based on Eq. (4), which retains terms only through order $k_0^3 \ln k_0$. Also shown are cross sections calculated in the first Born approximation (FBA) (dotted line) with a potential given by Eq. (2).

merically stable even when very stringent numerical criteria are imposed.

Studies of rotational excitation, especially at energies below the first vibrational threshold, are often performed in the rigid-rotor approximation, in which the internuclear separation is frozen at equilibrium. Although this approach can yield cross sections whose qualitative behavior is reliable, the effects of even the zero-point vibrational motion can be considerable [68]. For completeness, in Table II we also show MERT parameters from such a rigid-rotor calculation on $e\text{-N}_2$ scattering.

A. MERT-extrapolated K matrices

To illustrate the accuracy of the MERT extrapolation procedure for the $e\text{-N}_2$ system, we consider two crucial K -matrix elements. For calculating VLE momentum transfer cross sections, the most important matrix element is $\Sigma_g(0,0)$. In Fig. 2(a) we compare the MERT-extrapolated values for this element to their BFVCC counterparts, dem-

onstrating agreement to better than 1% from 0.2 eV down to 0.02 eV, the lowest energy at which we could converge the BFVCC calculations. At higher energies (not shown), this expansion is comparably accurate up to about 0.4 eV, beyond which it breaks down. This level of agreement characterizes the other important diagonal elements, $\Sigma_u(1,1)$, $\Pi_u(1,1)$, and $\Pi_g(2,2)$.

For calculating $\Delta j = \pm 2$ rotational cross sections, the diagonal $\Pi_u(1,1)$ and $\Sigma_u(1,1)$ elements are the most important except very near threshold. Here the scattering is dominated by the off-diagonal element $\Sigma_g(2,0)$. In Fig. 2(b) we compare BFVCC results for this matrix element to values from MERT extrapolations and as calculated in the FBA using the long-range potential (2). This figure compares two MERT expansions: the limited expansion (4), which includes only terms through order $k^3 \ln k$, and the extended expansion (8), which includes additional terms through order k^4 . Clearly, the limited expansion is accurate only very near the rotational threshold. As the energy increases, this expansion comes to qualitatively resemble the FBA values. The extended expansion Eq. (8), however, is accurate throughout the energy range from threshold to several times E_M .

The physical reason for improved accuracy of the extended expansion is suggested by the similarity of the limited expansion to the FBA values. As implemented with Eq. (2), the FBA K -matrix elements reflect only the long-range quadrupole and polarization interactions—not short- and intermediate-range effects. The limited MERT expansion Eq. (4) does incorporate these effects in the $k^3 \ln k$ term, which is proportional to the scattering length A (note that c_1 is independent of A for $\ell \neq \ell_0$). But for the $\Sigma_g(0,2)$ matrix element, in which the electron in the s -wave exit channel is fully exposed to short-range interactions, this incorporation of these interactions is inadequate. The addition of higher-order fitting coefficients c_3 and c_4 takes up the slack and yields a very accurate MERT expression. Of course, as $k \rightarrow 0$, both MERT expansions and the FBA results come into agreement.

B. Momentum-transfer cross sections

At low energies, the total $e\text{-N}_2$ momentum-transfer cross section, the sum of terms for elastic scattering and all energetically allowed excitations, is overwhelmingly dominated by the elastic ($j_0 \rightarrow j_0$) term, the contribution of which exceeds by two orders of magnitude that of the largest rotationally inelastic contribution. Hence $\sigma^{(m)}$ is determined to a great extent by the largest diagonal element of the K matrix, $\Sigma_g(0,0)$. In Fig. 2(a) we showed the MERT extrapolation of this element to be very accurate. Not surprisingly, then, we find in Fig. 3(a) that the $\sigma^{(m)}$ calculated from extrapolated K -matrix elements is essentially identical to that constructed from BFVCC elements.

One can, of course, generate MERT momentum-transfer cross sections directly from the scattering length using the expansion [36]

$$\begin{aligned} \sigma^{(m)} = & 4\pi \left(A^2 + \frac{4}{45} \bar{Q}^2 \right) + \frac{8\pi}{5} \left(2\pi A \bar{\alpha}_0 + \frac{\pi}{15} \bar{\alpha}_2 \bar{Q} \right) \\ & + 0.8625A \bar{Q}^2 + 0.06 \bar{Q}^3 \Big| k_0 + \left[-A \left(\frac{2}{45} \bar{\alpha}_2 \bar{Q} \right) \right] \end{aligned}$$

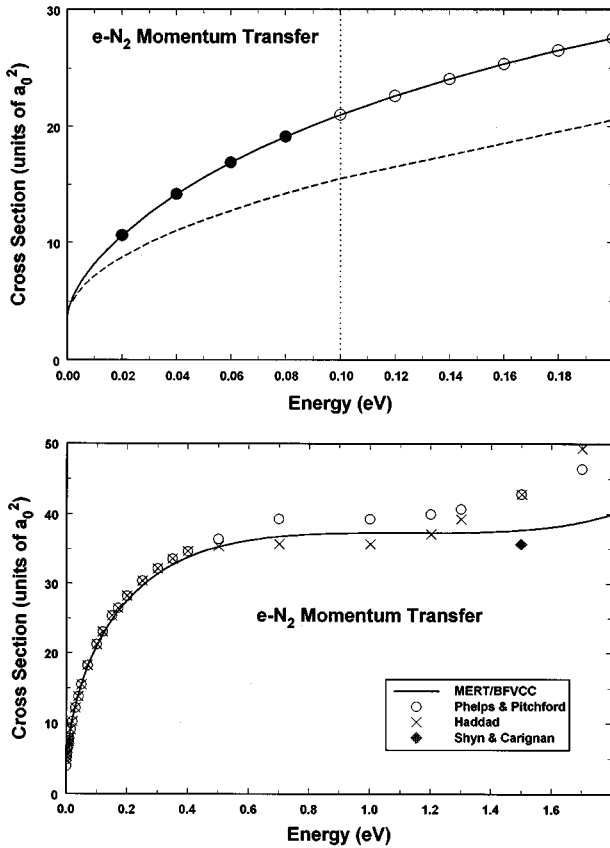


FIG. 3. (a) Total momentum-transfer cross sections for $e\text{-N}_2$ scattering from BFVCC calculations (open and closed circles), from a MERT extrapolation based on BFVCC K -matrix elements at $E \geq 0.1$ eV (solid line), and from the direct MERT expansion of this cross section, Eq. (19) (dashed curve). The open circles show BFVCC cross sections at the energies used to extract the MERT parameters; the closed circles denote BFVCC results below this energy, shown for comparison. (b) Comparison of composite MERT-BFVCC momentum-transfer cross sections to experimental values determined via from transport analyses by Haddad [21] (solid circles) and by Phelps and Pitchford [22] (dotted curve). Also shown is the crossed-beam result of Shyn and Carignan [24] (triangle).

$$\begin{aligned}
 & + 0.0034\bar{Q}^3) + \frac{4}{3}A^2\left(2\bar{\alpha}_0 + \frac{1}{5}\bar{Q}^2\right) - \bar{Q}^2(0.052\bar{\alpha}_0 \\
 & + 0.0186\bar{\alpha}_2) + 0.00112\bar{Q}^4\left]k_0^2 \ln k_0. \quad (19)
 \end{aligned}$$

Although an easier route to $\sigma^{(m)}$ than calculations from the BF MERT K matrix, use of Eq. (19) is also less accurate. To illustrate, we include in Fig. 3(a) cross sections obtained from this equation. Clearly, the higher-order analytic terms in the MERT K matrix play a significant role in this cross section over the whole energy range.

The BF MERT extrapolation enables the comparison of theoretical cross sections to those derived from transport analysis in Fig. 3(b). To this end we construct a ‘‘composite’’ cross-section set consisting of MERT-based values for energies $E \leq E_M$ and BFVCC values for $E \geq E_M$. The two swarm-based cross sections in this figure were determined by

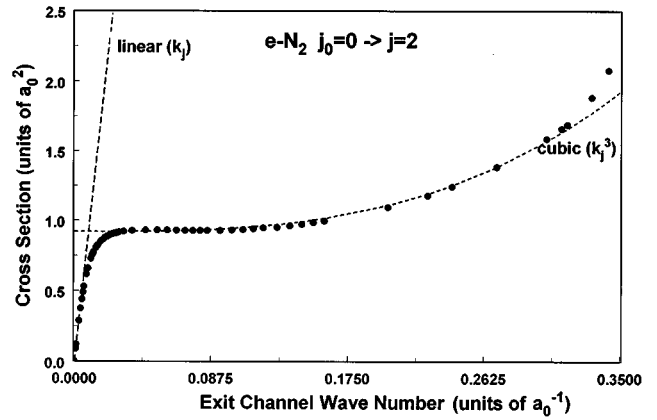


FIG. 4. Demonstration that the theoretical $e\text{-N}_2$ rotational $0 \rightarrow 2$ cross section (closed circles) obeys the threshold law Eq. (15). The dashed curves are, respectively, linear (long dash) and cubic (short dash) in the exit-channel wave number k_2 and, according to the threshold law for this excitation, correspond to outgoing s and p waves.

Haddad [21] and Phelps and Pitchford [22] in separate transport analyses of swarm data taken in pure N_2 . A more detailed test of the VLE theoretical $\sigma^{(m)}$, obtained by inserting it into the Boltzmann equation and using the resulting electron distribution function to calculate transport coefficients for comparison to measured data, will appear in Ref. [30].

C. Rotational excitation cross sections

Unlike $\sigma^{(m)}$, the rotational cross sections $\sigma_{j_0 \rightarrow j}^{(r)}(E)$ at very low energies are significantly influenced by scattering in more than one symmetry. The threshold laws (14) and (15), which apply at energies sufficiently near the rotational threshold, shed light on the dominant exit-channel partial wave order (ℓ) at these energies. In Fig. 4 we compare the dependence of the $0 \rightarrow 2$ cross section on exit-channel wave number k_2 [see Eq. (12)] with the predictions of Eq. (15). As E_0 approaches threshold and k_0 approaches zero, $\sigma_{0 \rightarrow 2}^{(r)}$ goes to zero as the first power of k_2 , corresponding to an s -wave exit channel—as expected from the aforementioned dominance of the $\Sigma_g(2,0)$ K -matrix element. With a slight increase in energy, however, this dependence switches to k_2^3 , corresponding to a p -wave exit channel. At these energies, scattering is strongly influenced by the $\Pi_u(1,1)$ and, to a lesser extent, the $\Sigma_u(1,1)$ elements. So, except *very* near threshold, all three of these symmetries must be represented accurately to produce PC rotational cross sections.

These findings, together with the sensitivity of $\Sigma_g(2,0)$ to short-range interactions demonstrated in Fig. 2(b), suggest that the limited MERT expansion Eq. (4) will not provide sufficient accuracy to ensure precise rotational cross sections throughout the energy range of interest. Sure enough, Fig. 5 shows that the higher-order fitting coefficients of Eq. (8) are required to accurately reproduce the $0 \rightarrow 2$ cross section.

D. Anomalous behavior of rotational cross sections in transport analysis

The MERT-extrapolated rotational cross sections examined above are sufficiently accurate to warrant their use in an

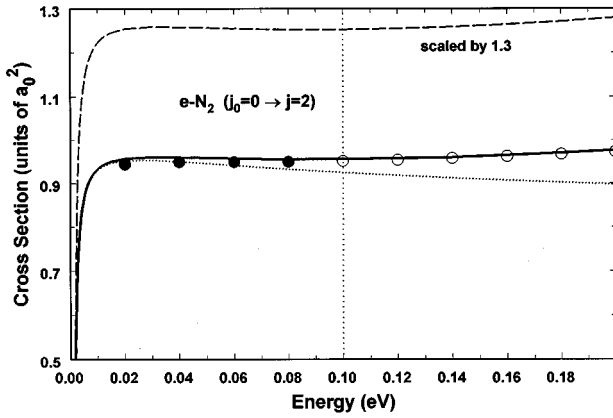


FIG. 5. Rotational cross sections for the $0 \rightarrow 2$ excitation from BFVCC scattering calculations and from MERT extrapolations based on BFVCC K -matrix elements at $E \geq 0.1$ eV (solid and dotted curves). The open circles show BFVCC results at energies used to extract the MERT parameters; the closed circles denote results below this energy. The cross sections based on MERT K matrices were obtained in two separate extrapolations, one to order k^3 (dotted curve), the other including coefficients for k^3 and k^4 terms (solid curve). Also shown are the BFVCC-MERT cross sections scaled by 1.3 to account for inaccuracies in the quadrupole moment (see text).

inquiry into the long-standing enigma concerning e - N_2 transport analysis described in Sec. I—that this analysis yields transport coefficients within experimental error bars only when based on the QBA $\Delta j = 2$ rotational cross sections. The behavior of the $0 \rightarrow 2$ cross section in Fig. 5 is typical of those that participate in this analysis. After its sharp rise from zero at threshold, this cross section exhibits very little variation with scattering energy until E_0 exceeds 0.2 eV. This energy dependence appears more akin to that of the QBA cross section that the presumably more accurate QPBA result—which, as its acronym indicates, includes an interaction (polarization) that the QBA neglects. This resemblance is explored further in the comparison in Fig. 6 of these two Born results to the composite MERT-BFVCC cross sections.

The QBA cross section for a $\Delta j = \pm 2$ transition in a homonuclear molecule is [23]

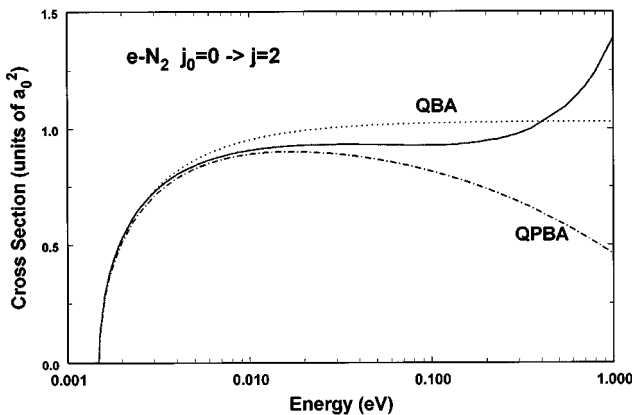


FIG. 6. Comparison of BFVCC-MERT $0 \rightarrow 2$ rotational e - N_2 cross sections (solid curve) with values calculated in the quadrupole Born (dotted curve) and quadrupole-polarized Born approximations (dashed curve), Eqs. (20) and (22), respectively.

$$\text{QBA } \sigma_{j_0 \rightarrow j}^{(r)} = \frac{8\pi}{15} \frac{k_j}{k_0} \bar{Q}^2 F_{\pm}(j_0), \quad (20)$$

where the factor $F_{\pm}(j_0)$ discriminates inelastic from super-elastic scattering,

$$F_{\pm}(j_0) \equiv \begin{cases} \frac{(j_0+1)(j_0+2)}{(2j_0+1)(2j_0+3)} & (j_0 \rightarrow j_0+2) \\ \frac{j_0(j_0-1)}{(2j_0-1)(2j_0+1)} & (j_0 \rightarrow j_0-2). \end{cases} \quad (21)$$

This approximation is strictly valid only in the $k_j \rightarrow 0$ limit, where the strong centrifugal barrier in the d -wave entrance channel [as manifested in the dominant $\Sigma_g(0,2)$ K -matrix element] guarantees very weak scattering at very long range—conditions that validate retention of only the quadrupole interaction. Just above threshold, significant scattering occurs in channels with (weaker) p -wave barriers and the long-range polarization interaction begins to play a role. This interaction, therefore, should be taken into account—as it is in the QPBA expression [25]

$$\text{QPBA } \sigma_{j_0 \rightarrow j}^{(r)} = \text{QBA } \sigma_{j_0 \rightarrow j}^{(r)} + \frac{\pi^2}{30} \frac{k_j}{k_0} \left[Q \bar{\alpha}_2 \frac{3k_0^2 + k_j^2}{k_j} + \frac{9\pi}{64} \bar{\alpha}_2^2 (k_0^2 + k_j^2) \right] F_{\pm}(j_0). \quad (22)$$

Note that Eq. (22) corrects Eq. (20) with an additional term whose dominant dependence on k_j is k_j^3 , consistent with the threshold law for $\ell = 1$, as required according to Fig. 4. In e - N_2 scattering, the effect of this correction term is especially dramatic because of a partial cancellation in the long-range potential due to the opposite signs of \bar{Q} and $\bar{\alpha}_2$; this effect can be seen in the comparison of two Born $0 \rightarrow 2$ cross sections in Fig. 6. This line of reasoning highlights the anomalous nature of the agreement in shape of the MERT-BFVCC rotational cross sections and those of the QBA theory.

This agreement, however, is misleading. The apparent anomaly is explained by the demonstration in Figs. 2(b) and 5 that the short- and intermediate-range interactions (static, exchange, intermediate-range polarization, and bound-free correlation) significantly affect K -matrix elements that are important to $\sigma_{0 \rightarrow 2}^{(r)}$ at these energies. As shown in Fig. 5, the effect of adequately representing these interactions, through the coefficients c_3 and c_4 in Eq. (8), is to increase this cross section. Coincidentally, the energy dependence of the resulting more accurate rotational cross section more closely resembles that of the QBA theory than of the QPBA theory.

It is important that the results in Fig. 6 not be misconstrued to mean either that the QBA theory accurately reflects the physics of rotational excitation at these energies, or that one can use it with impunity for other systems. Quite the contrary. Both the QBA and QPBA theories neglect completely short- and intermediate-range interactions; neither, therefore, correctly incorporates physical effects that are important at energies ranging from slightly above threshold to several tenths of an eV. The coincidental concurrence between the shapes of the QBA and MERT-BFVCC rotational

cross sections explains why in prior transport analysis of swarm data in pure N_2 and in N_2 -rare-gas mixtures, only QBA rotational cross sections yielded transport coefficients that agreed with measured data [21]. The coincidental nature of this agreement is the crucial point; no such agreement should be anticipated for other electron-molecule systems.

In conclusion, we should note that—notwithstanding the importance of interactions other than the long-range quadrupole—at very low energies $\sigma_{0 \rightarrow 2}^{(r)}$ remains very sensitive to the value of the quadrupole moment \bar{Q} . Our MERT-BFVCC cross sections correspond to $\bar{Q} = -0.961ea_0^2$, which may be compared to the experimental values of $\bar{Q} = -(1.04 \pm 0.07)ea_0^2$ obtained from electric-field-gradient-induced birefringence measurements [54], and $-1.15ea_0^2$ extracted from far-infrared spectra [69].

Our theoretical quadrupole moment is too small because it is based on a near-Hartree-Fock representation of the $X^1\Sigma_g$ ground electronic state of N_2 . A more accurate electronic function would have produced a different quadrupole moment. For example, the fourth-order perturbation theory calculations of Maroulis and Thakkar [70] give $\bar{Q} = -1.146ea_0^2$, while the multiconfiguration self-consistent-field calculations of Ermler and Huang [71] yield $-1.25ea_0^2$. However, unanimity about the theoretical dependence of $Q(R)$ on internuclear separation R seems elusive. Table I in Liu, Lie, and Liu [72], which collects various theoretical values of $Q(R=2.068a_0)$, displays configuration-interaction values ranging from $-0.98ea_0^2$ to $-1.25ea_0^2$. (Our near-Hartree-Fock value at this internuclear separation is $-0.902ea_0^2$.) Averaging these values over the ground vibrational state would increase them by about 6%.

Because of the aforementioned sensitivity of $\sigma_{j_0 \rightarrow j}^{(r)}$ to \bar{Q} , this uncertainty about the quadrupole moment has significant consequences for transport analysis based either on QBA theory or the present MERT-BFVCC rotational cross sections. The MERT expansion (4) shows that the dominant dependence of $\Delta j = \pm 2$ cross sections on the quadrupole moment is \bar{Q}^2 . This holds from threshold to several tenths of an eV—precisely the energy range in which the drift velocity is most sensitive to rotational excitation. This observation suggests a crude (but efficient) way to correct our rotational cross sections: simply scale them by the square of the ratio of the experimental to theoretical quadrupole moment. If, for example, one takes as the experimental value $1.1ea_0^2$, then the cross sections in Fig. 5 should be multiplied by $|1.1/0.961|^2 = 1.3$. The result of this scaling, shown in Fig. 5, illustrates the sensitivity of these cross sections to \bar{Q} . As detailed in Ref. [29], these scaled theoretical rotational cross sections, when inserted into the Boltzmann equation, yield transport coefficients within the 1% error bars of the most recent swarm experiments. This, we believe, explains the apparent enigma with respect to this scattering process.

Nevertheless, in addition to being somewhat unrefined, this scaling correction suffers from uncertainty about the experimental value of \bar{Q} . But it is unarguably easier than repeating the current scattering calculations with a configuration-interaction (CI) target function—a CPU-intensive effort that would also be plagued by the aforementioned uncertainties about the CI value of this molecular con-

stant. In any case, no such scaling is required (or appropriate) for the momentum transfer cross section, the total cross section, or rotational cross sections above a few tenths of an eV—none of which are similarly dominated by the long-range quadrupole interaction.

E. Fitted cross sections

To facilitate their future use, we here present our composite MERT-BFVCC cross sections in a user-friendly form. The threshold laws for $\sigma^{(m)}$ and $\sigma_{j_0 \rightarrow j}^{(r)}$ prescribe the dependence of these quantities on the exit-channel wave number k_j . Thus we can use these laws to construct series expansions of these cross sections, and determine the required expansion coefficients via linear regression analysis [73].

To determine which terms to include in this fit, we turn to the BF-MERT expansion of the momentum transfer cross section, Eq. (19). The leading k_0 -dependent terms in this expression are proportional to k_0 and $k_0^2 \ln k_0$. Translated into the incident projectile energy $E_0 = k_0^2/2$, these terms yield factors proportional to $\sqrt{E_0}$, E_0 , and $E_0 \ln E_0$. As noted in the discussion of Eq. (19) and illustrated in Fig. 3(a), this direct MERT expansion of $\sigma^{(m)}$ is not valid over the entire energy range from 0.002 to 1.25 eV. Thus instead we fit our MERT-BFVCC cross sections, augmenting these terms with one proportional to $k_0^4 \propto E_0^2$ to accommodate the high end of this range.

At zero energy, $\sigma^{(m)}$ should reduce to the value $4\pi A^2$, which, for our scattering length $A = 0.420a_0$ equals $2.2167a_0^2$. However, because BF MERT entails the FNO approximation, the total momentum-transfer cross section (at any energy) includes contributions from all rotational excitations, whether or not they actually correspond to open channels; these contributions are nonzero because, as noted in Sec. II, they do not approach zero at their respective excitation thresholds. This results in a zero-energy limit that is incorrect by an amount $16\pi\bar{Q}^2/45$, which for our e - N_2 calculations equals $1.031a_0^2$. To correct this slight mismatch in the present fit, we simply replace the zeroth-order value by its correct limit $4\pi A^2$. Doing so yields the following fit for the total momentum-transfer cross section (in a_0^2) as a function of incident energy E_0 (in eV):

$$\sigma^{(m)} = 2.2167 + 29.2988E_0^{1/2} - 44.6748E_0 \ln E_0 - 20.3865E_0 + 25.4971E_0^2. \quad (23)$$

This fit reproduces our MERT-BFVCC momentum-transfer cross sections to better than 1% from zero to 1.25 eV.

Similarly, we can use the known behavior of the rotational cross section to devise a fit to our composite MERT-BFVCC values for $\Delta j = 2$ transitions, which, as noted above, are the only appreciable excitations below the resonance region from about 1.5 to 4.0 eV. (Cross sections for deexcitation can be calculated from these using detailed balance.) As E_0 decreases toward threshold ϵ_j , this rotational cross section approaches the QBA form (20). Hence we can write it in a form that introduces an ancillary function $f_{j_0 \rightarrow j}(E_0)$ which goes to zero at threshold, viz.,

$$\sigma_{j_0 \rightarrow j}^{(r)}(E_0) = {}^{\text{QBA}}\sigma_{j_0 \rightarrow j}^{(r)}(E_0)[1 + f_{j_0 \rightarrow j}(E_0)], \quad (24)$$

TABLE III. Coefficients in the ancillary function $f_{j_0 \rightarrow j}(E_0)$ of Eq. (25) used to fit theoretical e -N₂ rotational cross sections for $j_0 \rightarrow j_0 + 2$ transitions. These are coefficients of powers of the incident energy E minus the threshold energy ϵ_j (both in eV). The analytic forms obtained by inserting these functions into Eq. (24) for $\sigma_{j_0 \rightarrow j}^{(r)}(E)$ reproduce to within 1% our calculated cross sections from threshold to 1.25 eV. (Threshold energies are based on constants in Ref. [66].)

j_0	ϵ_j (eV)	d_1	d_2	d_4
0	0.001 480	-2.0216	10.8604	18.2194
1	0.002 466	-1.8734	9.2870	39.6345
2	0.003 453	-1.9283	9.8817	32.3389
3	0.004 440	-1.9151	9.8909	31.3904
4	0.005 426	-1.9101	9.9038	31.0499
5	0.006 413	-1.8976	9.8645	31.1314
6	0.007 399	-1.8791	9.7873	31.4314
7	0.008 386	-1.8563	9.6436	32.4237
8	0.009 373	-1.8351	9.5712	32.5957
9	0.010 359	-1.8100	9.4427	33.3092
10	0.011 346	-1.7805	9.2820	34.2476
11	0.012 334	-1.7615	9.1977	34.6676
12	0.013 319	-1.7679	9.2964	34.0475

and need to fit only the ancillary function to theoretical data. Note that the QBA cross section goes to zero as k_j , in conformity with the threshold law (15) for the s -wave-dominated exit channel, as illustrated in Fig. 4.

Swarm experiments typically require $\Delta_j = 2$ cross sections for a range of initial states j_0 . For example, the recent swarm experiments in N₂-Ne mixtures, which were performed at 78.6 K, require cross sections for $j_0 = 0, 1, \dots, 12$. We have generated and fit the ancillary function for these transitions, using the form

$$f(E_0) = d_1 \sqrt{E_0 - \epsilon_j} + d_2(E_0 - \epsilon_j) + d_4(E_0 - \epsilon_j)^2, \quad (25)$$

and obtain the coefficients in Table III. This fit reproduces our SANR-corrected MERT-BFVCC cross sections to better than 1% from threshold to 1.25 eV. If cross sections for higher j_0 are required, say for analysis of experiments at higher temperatures, they can be generated from the data in Table III using scaling relations such as those described in Ref. [74].

IV. CONCLUSION

The principal theoretical result of this study is the BF-MERT extrapolation procedure summarized in Fig. 1. The principal practical results are the fits (23) and (24) to our composite MERT-BFVCC e -N₂ momentum-transfer and rotational cross sections. These fits can be used, together with scaling formulas if necessary [74], to generate $\sigma^{(m)}$ or any desired $\sigma_{j_0 \rightarrow j}^{(r)}$ for $\Delta_j = 2$ at energies below about 1.25 eV. Above this energy, rotational excitation is controlled by the 2.4-eV shape resonance, the shapes of these cross sections differ from those off resonance, and $\Delta_j = 4$ transitions become appreciable. In addition to the validity of MERT for $E \leq E_M$, the assumptions underlying the present results are those of the BFVCC scattering calculations for $E \geq 0.1$ eV—

primarily the FNO approximation, use of a near-Hartree-Fock electronic function for the target, and simplifications in the exchange and polarization constituents of the interaction potential; we discussed these assumptions in detail in Ref. [35].

The principal conceptual result is the resolution of the long-standing enigma concerning in swarm determination of e -N₂ rotational cross sections (see Fig. 6 and the accompanying discussion). This resolution brings additional coherence to a long-term project in which we have been assessing both theory and transport analysis for electron-molecule scattering. Our goal is to generate benchmark cross sections for a few typical electron-molecule systems—a database on which theory and experiment can agree to high precision. Prior work on low-energy e -H₂ scattering has accomplished this goal for rotational excitation, determining cross sections on a par with those for low-energy e -He cross sections [75]. As elaborated in the companion paper Ref. [29], the present study brings e -N₂ rotational cross sections to this level of agreement. The situation concerning vibrational excitation, of both H₂ and N₂ remains, alas, more recalcitrant [13].

In considering the extension of the present approach to a calculation of very-low-energy momentum transfer and rotational cross sections for other types of electron-molecule systems (e.g., scattering from polar and polyatomic targets), the primary concerns are two. First, BF-MERT expressions for the system of interest must be available or derived. Second, the BFVCC (or, if appropriate, BF rigid rotor) scattering equations must be solvable at a few energies at the upper limit of the range of validity of BF-MERT. A more detailed discussion of MERT for various systems can be found in Sec. IV B of Ref. [33].

To conclude, it is perhaps worth setting the present scheme in a practical perspective. The only computationally demanding step is solving the BFVCC scattering equations at a few energies above 0.1 eV. While we used fully converged five-(vibrational)-state BFVCC K matrices, one could render this step considerably simpler with little loss of accuracy. For example, if only rotationally inelastic processes are of interest, one can avoid vibrational coupling altogether by using the rigid-rotor approximation. This entails solving fixed-nuclei scattering equations at the equilibrium geometry, and is quite standard in the repertoire of modern electron-molecule theory. Only a few such calculations need be performed to obtain parameters for the MERT extrapolation. All subsequent steps in the generation of VLE cross sections—fitting the K -matrix elements, MERT extrapolation to lower energies, the rotational frame transformation, and correction of the LAB-CAM T -matrix elements near threshold—involve easily programmed, very fast, numerically stable calculations that can be executed on a modest personal computer or work station.

ACKNOWLEDGMENTS

We would like to acknowledge useful discussions with Dr. Ilya Fabrikant, Dr. Robert Crompton, and Dr. Malcolm Elford concerning various aspects of this work. W.A.I. would like to thank the Department of Education. We all gratefully acknowledge the support of the National Science Foundation under Grant No. PHY-9408977.

- [1] S. Wong and L. Dube, *Phys. Rev. A* **17**, 570 (1978).
- [2] A. Chutjian, *Electronic and Atomic Collisions*, edited by W. R. McGillivray, I. E. McCarthy, and M. C. Standage (Hilger, Bristol, 1992), pp. 127–38.
- [3] H. Ibach, *J. Electron Spectrosc. Relat. Phenom.* **64/65**, 819 (1993).
- [4] D. Field, J. P. Ziesel, P. M. Guyon, and T. R. Govers, *J. Phys. B* **17**, 4565 (1984); D. Field, S. L. Lunt, G. Mrotzek, J. Randell, and J. P. Ziessel *ibid.* **24**, 3497 (1991); J. Randell, S. L. Lunt, G. Mrotzek, J.-P. Ziessel, and D. Field, *ibid.* **27**, 2369 (1994).
- [5] M. Matsuzawa, in *Rydberg States of Atoms and Molecules*, edited by R. F. Stebbings and F. B. Dunning (Cambridge University Press, New York, 1983), Chap. 8.
- [6] F. B. Dunning *J. Phys. B* **28**, 1645 (1995).
- [7] *Electronic and Atomic Collisions: Processes at Low and Ultralow Energies*, edited by H. Hotop and M.-W. Ruf, European Research Conference 1994 Series (European Science Foundation, Giens, 1994).
- [8] M. A. Morrison, R. W. Crompton, B. C. Saha, and Z. Lj. Petrović, *Aust. J. Phys.* **40**, 239 (1987).
- [9] For a summary, see R. W. Crompton and M. A. Morrison, in *Swarm Studies and Inelastic Electron-Molecule Scattering*, edited L. C. Pitchford, V. McKoy, A. Chutjian, and S. Trajmar (Springer-Verlag, Berlin, 1986).
- [10] B. Schmidt, *Comments At. Mol. Phys.* **28**, 379 (1993); B. Schmidt, K. Berkham, B. Götz, and M. Müller, *Phys. Scr.* **T53**, 30 (1994).
- [11] L. G. H. Huxley and R. W. Crompton, *The Diffusion and Drift of Electrons in Gases* (Wiley, New York, 1974).
- [12] L. G. H. Huxley and R. W. Crompton, in *Atomic and Molecular Processes*, edited by D. R. Bates (Academic, New York, 1962), Chap. 10; R. W. Crompton, *Adv. Electron. Electron Phys.* **27**, 1 (1969); R. W. Crompton, *Aust. Phys.* **25**, 146 (1988); K. Kumar, H. R. Skullerud, and R. E. Robson, *Aust. J. Phys.* **33**, 343 (1980); R. W. Crompton (unpublished); in *Second Australia-Japan Workshop on Gaseous Electrons and Its Applications, Abstracts of Papers* (Toganso Yotemba, Japan, 1990), p. 37.
- [13] R. W. Crompton and M. A. Morrison, *Aust. J. Phys.* **46**, 203 (1993).
- [14] Stephen J. Buckman, M. J. Brunger, D. S. Newman, G. Snitchler, S. Alston, D. W. Norcross, Michael A. Morrison, B. C. Saha, G. Danby, and W. K. Trail, *Phys. Rev. Lett.* **65**, 3253 (1990).
- [15] Weiguo Sun, Michael A. Morrison, William A. Isaacs, Wayne K. Trail, Dean T. Alle, R. J. Gulley, Michael J. Brennan, and Stephen J. Buckman, *Phys. Rev. A* **52**, 1229 (1995).
- [16] N. F. Lane, *Rev. Mod. Phys.* **52**, 29 (1980).
- [17] W. Domcke, *Phys. Rep.* **208**, 98 (1991).
- [18] S. Trajmar, D. F. Register, and A. J. Chutjian, *Phys. Rep.* **97**, 220 (1983).
- [19] Y. Itikawa, M. Hayashi, A. Ichimura, K. Onda, K. Sakimoto, K. Takayanagi, M. Nakamura, H. Nishimura, and T. Takayanagi, *J. Phys. Chem. Ref. Data* **15**, 985 (1986).
- [20] L. S. Frost and A. V. Phelps, *Phys. Rev.* **127**, 1621 (1962); A. G. Engelhardt, A. V. Phelps, and C. G. Risk, *ibid.* **135**, A1556 (1964); D. Levron and A. V. Phelps, *Bull. Am. Phys. Soc.* **24**, 129 (1979); K. Tachibana and A. V. Phelps, *J. Chem. Phys.* **71**, 3544 (1979); H. Tagashira, T. Tanaguchi, and T. Sakai, *J. Phys. D* **13**, 235 (1980).
- [21] G. Haddad, *Aust. J. Phys.* **37**, 487 (1984).
- [22] A. V. Phelps and L. C. Pitchford, *Phys. Rev. A* **31**, 2932 (1985); see also A. V. Phelps and L. C. Pitchford, JILA Data Center Report No. 26, 1985 (unpublished).
- [23] E. Gerjuoy and S. Stein, *Phys. Rev.* **97**, 1671 (1955).
- [24] T. W. Shyn and G. R. Carignan, *Phys. Rev. A* **22**, 923 (1980).
- [25] A. Dalgarno and R. J. Moffett, *Proc. Natl. Acad. Sci. India* **33**, 511 (1963).
- [26] D. H. Sampson and R. C. Mjolsness, *Phys. Rev.* **140**, A1466 (1965).
- [27] K. Onda, *J. Phys. Soc. Jpn.* **54**, 4544 (1985).
- [28] M. A. Morrison, B. C. Saha, and T. L. Gibson, *Phys. Rev. A* **36**, 3682 (1987).
- [29] A. G. Robertson, M. T. Elford, R. W. Crompton, Michael A. Morrison, W. Sun, and W. K. Trail, *Aust. J. Phys.* (to be published).
- [30] M. A. Morrison, *Aust. J. Phys.* **36**, 239 (1983).
- [31] M. A. Morrison, in *Electron- and Photon-Molecule Collisions*, edited by T. N. Rescigno, B. V. McKoy, and B. I. Schneider (Plenum, New York, 1979).
- [32] M. A. Morrison, A. N. Feldt, and D. A. Austin, *Phys. Rev. A* **29**, 2518 (1984).
- [33] M. A. Morrison, *Adv. At. Mol. Phys.* **24**, 51 (1988).
- [34] I. Shimamura, in *Electron-Molecule Collision*, edited by I. Shimamura and K. Takayanagi (Plenum, New York, 1984), Chap. 2.
- [35] M. A. Morrison and W. Sun, in *Computational Methods for Electron-Molecule Collisions*, edited by W. Muo and F. A. Gianturco (Plenum, New York, 1995), Chap. 6.
- [36] I. I. Fabrikant, *J. Phys. B* **17**, 4223 (1984).
- [37] W. A. Isaacs and M. A. Morrison, *J. Phys. B* **25**, 703 (1992).
- [38] W. A. Isaacs and M. A. Morrison, *Phys. Rev. A* **53**, 4215 (1996).
- [39] E. S. Chang and U. Fano, *Phys. Rev. A* **6**, 173 (1972).
- [40] A. N. Feldt and M. A. Morrison, *Phys. Rev. A* **29**, 401 (1984).
- [41] T. F. O'Malley, *Phys. Rev.* **130**, 1020 (1963).
- [42] T. F. O'Malley, L. Spruch, and L. Rosenberg, *J. Math. Phys.* **2**, 491 (1961); T. F. O'Malley, L. Spruch, and L. Rosenberg, *Phys. Rev. A* **125**, 1300 (1962).
- [43] T. F. O'Malley, *Adv. At. Mol. Phys.* **7**, 223 (1971).
- [44] T. F. O'Malley, *Phys. Rev. A* **134**, A1188 (1964).
- [45] T. F. O'Malley, *Phys. Rev. A* **137**, 1668 (1965); **150**, 14 (1966).
- [46] S. J. Buckman and J. Mitroy, *Aust. J. Phys.* **22**, 1365 (1989).
- [47] J. R. Taylor, *Scattering Theory* (Wiley, New York, 1972).
- [48] N. Chandra and A. Temkin, *Phys. Rev. A* **13**, 188 (1976).
- [49] W. N. Sams and D. J. Kouri, *J. Chem. Phys.* **51**, 4809 (1969).
- [50] M. A. Morrison, N. F. Lane, and L. A. Collins, *Phys. Rev. A* **15**, 2186 (1977).
- [51] M. A. Morrison, N. F. Lane, and L. A. Collins, *Phys. Rev. A* **15**, 2186 (1977).
- [52] T. L. Gibson and M. A. Morrison, *J. Phys. B* **15**, L221 (1982); *Phys. Rev. A* **29**, 2497 (1984).
- [53] T. M. Miller and B. Bederson, *Adv. At. Mol. Phys.* **13**, 1 (1978).
- [54] A. D. Buckingham, C. Graham, and J. H. Williams, *Mol. Phys.* **49**, 703 (1983).
- [55] R. H. Orcutt and R. H. Cole, *J. Chem. Phys.* **46**, 697 (1967).
- [56] A. C. Newell and R. C. Baird, *J. Appl. Phys.* **36**, 3751 (1965).
- [57] N. J. Bridge and A. D. Buckingham, *Proc. R. Soc. London Ser. A* **295**, 334 (1966).

- [58] I. Cernusak, G. H. F. Diercksen, and A. J. Sadlej, *Chem. Phys.* **108**, 45 (1986).
- [59] S. R. Langhoff, C. W. Bauschlicher, Jr., and D. P. Chong, *J. Chem. Phys.* **78**, 5287 (1993).
- [60] A. Temkin, *Phys. Rev.* **107**, 1004 (1957).
- [61] M. A. Morrison and B. C. Saha, *Phys. Rev. A* **34**, 2786 (1986).
- [62] S. Hara, *J. Phys. Soc. Jpn.* **22**, 710 (1967); **27**, 1262 (1969).
- [63] M. A. Morrison and L. A. Collins, *Phys. Rev. A* **17**, 918 (1978); **23**, 127 (1981); T. L. Gibson and M. A. Morrison, *J. Phys. B* **14**, 727 (1981); M. A. Morrison and L. A. Collins, *Phys. Rev. A* **25**, 1764 (1982).
- [64] M. E. Rose, *Elementary Theory of Angular Momentum* (Wiley, New York, 1957).
- [65] A. Temkin, K. V. Vasavada, E. S. Chang, and A. Silver, *Phys. Rev. A* **186**, 57 (1969); S. Hara, *J. Phys. Soc. Jpn.* **27**, 1592 (1969).
- [66] A. A. Radzig and B. Smirnov, *Reference Data on Atoms, Molecules, and Ions* (Springer-Verlag, New York, 1985).
- [67] J. N. Bardsley and R. K. Nesbet, *Phys. Rev. A* **8**, 203 (1973).
- [68] W. K. Trail, M. A. Morrison, W. A. Isaacs, and B. C. Saha, *Phys. Rev. A* **41**, 4868 (1990).
- [69] G. Birnbaum and E. R. Cohen, *Mol. Phys.* **32**, 161 (1976).
- [70] G. Maroulis and A. J. Thakkar, *J. Phys. B* **20**, L551 (1987).
- [71] P. C. Engelking and D. R. Herrick, *Phys. Rev. A* **30**, 750 (1984).
- [72] J. W. Liu, G. C. Lie, and B. Liu, *J. Phys. B* **20**, 2853 (1987).
- [73] S. Wolfram, *Mathematica: A System for Doing Mathematics by Computer*, 2nd ed. (Addison-Wesley, New York, 1991).
- [74] W. K. Trail and M. A. Morrison (unpublished).
- [75] R. K. Nesbet, *Phys. Rev. A* **20**, 58 (1978).